PHYSICAL REVIEW D **78,** 063544 (2008)

Nonperturbative quantum de Sitter universe

J. Ambjørn,[1,3,*] A. Görlich,[2,+] J. Jurkiewicz,[2,‡] and R. Loll[3,§]

[1]*The Niels Bohr Institute, Copenhagen University, Blegdamsvej 17, DK-2100 Copenhagen Ø, Denmark*
[2]*Institute of Physics, Jagellonian University, Reymonta 4, PL 30-059 Krakow, Poland*
[3]*Institute for Theoretical Physics, Utrecht University, Leuvenlaan 4, NL-3584 CE Utrecht, The Netherlands*

(Received 29 July 2008; published 26 September 2008)

The dynamical generation of a four-dimensional classical universe from nothing but fundamental quantum excitations at the Planck scale is a long-standing challenge to theoretical physicists. A candidate theory of quantum gravity which achieves this goal without invoking exotic ingredients or excessive fine-tuning is based on the nonperturbative and background-independent technique of causal dynamical triangulations. We demonstrate in detail how in this approach a macroscopic de Sitter universe, accompanied by small quantum fluctuations, emerges from the full gravitational path integral, and how the effective action determining its dynamics can be reconstructed uniquely from Monte Carlo data. We also provide evidence that it may be possible to penetrate to the sub-Planckian regime, where the Planck length is large compared to the lattice spacing of the underlying regularization of geometry.

DOI: 10.1103/PhysRevD.78.063544 PACS numbers: 98.80.Qc, 04.60.Gw, 04.60.Nc

I. INTRODUCTION

A major unsolved problem in theoretical physics is to reconcile the classical theory of general relativity with quantum mechanics. Of the numerous attempts, some have postulated new and so far unobserved ingredients, while others have proposed radically new principles governing physics at the as yet untested Planckian energy scale. Here we report on a much more mundane approach using only standard quantum field theory. In a sum-over-histories approach we will attempt to define a nonperturbative quantum field theory which has as its infrared limit ordinary classical general relativity and at the same time has a nontrivial ultraviolet limit. From this point of view it is in the spirit of the renormalization group approach, first advocated long ago by Weinberg [1], and more recently substantiated by several groups of researchers [2]. However, it has some advantages compared to the renormalization group approach in that it allows us to study (numerically) certain geometric observables which are difficult to handle analytically.

We define the path integral of quantum gravity nonperturbatively using the lattice approach known as *causal dynamical triangulations* (CDT) as a regularization. In Sec. II we give a short description of the formalism, providing the definitions which are needed later to describe the measurements. CDT establishes a nonperturbative way of performing the sum over four-geometries (for more extensive definitions, see [3,4]). It sums over the class of piecewise linear four-geometries which can be assembled from four-dimensional simplicial building blocks of link length a, such that only *causal* spacetime histories are included. The continuum limit of such a lattice theory should ideally be obtained as for QCD defined on an ordinary fixed lattice, where for an observable $\mathcal{O}(x_n)$, x_n denoting a lattice point, one can measure the correlation length $\xi(g_0)$ from

$$-\log(\langle \mathcal{O}(x_n)\mathcal{O}(y_m)\rangle) \sim |n-m|/\xi(g_0) + o(|n-m|). \quad (1)$$

A continuum limit of the lattice theory may then exist if it is possible to fine-tune the bare coupling constant g_0 of the theory to a critical value g_0^c such that the correlation length goes to infinity, $\xi(g_0) \to \infty$. Knowing how $\xi(g_0)$ diverges for $g_0 \to g_0^c$ determines how the lattice spacing a should be taken to zero as a function of the coupling constants, namely

$$\xi(g_0) = \frac{1}{|g_0 - g_0^c|^\nu}, \qquad a(g_0) = |g_0 - g_0^c|^\nu. \quad (2)$$

The challenge when searching for a *field theory* of quantum gravity is to find a theory which behaves in this way. The challenge is threefold: (i) to find a suitable nonperturbative formulation of such a theory which satisfies a minimum of reasonable requirements, (ii) to find observables which can be used to test relations like (1), and (iii) to show that one can adjust the coupling constants of the theory such that (2) is satisfied. Although we will focus on (i) in what follows, let us immediately mention that (ii) is notoriously difficult in a theory of quantum gravity, where one is faced with a number of questions originating in the dynamical nature of geometry. What is the meaning of distance when integrating over all geometries? How do we attach a meaning to local spacetime points like x_n and y_n? How can we define at all local, diffeomorphism-invariant quantities in the continuum which can then be translated to the regularized (lattice) theory?—What we

*ambjorn@nbi.dk
+atg@th.if.uj.edu.pl
‡jurkiewicz@th.if.uj.edu.pl
§r.loll@phys.uu.nl

want to point out here is that although (i)–(iii) are standard requirements when relating critical phenomena and (Euclidean) quantum field theory, gravity *is* special and may require a reformulation of (part of) the standard scenario sketched above. We will return to this issue when we discuss our results in Sec. VIII.

Our proposed nonperturbative formulation of four-dimensional quantum gravity has a number of nice features. First, it sums over a class of piecewise linear geometries, which—as usual—are described without the use of coordinate systems. In this way we perform the sum over geometries directly, avoiding the cumbersome procedure of first introducing a coordinate system and then getting rid of the ensuing gauge redundancy, as one has to do in a continuum calculation. Our underlying assumptions are that (1) the class of piecewise linear geometries is in a suitable sense dense in the set of all geometries relevant for the path integral (probably a fairly mild assumption), and (2) we are using a correct measure on the set of geometries. This is a more questionable assumption since we do not even know whether such a measure exists. Here one has to take a pragmatic attitude in order to make progress. We will simply examine the outcome of our construction and try to judge whether it is promising.

Second, our scheme is background independent. No distinguished geometry, accompanied by quantum fluctuations, is put in by hand. If the CDT-regularized theory is to be taken seriously as a potential theory of quantum gravity, there has to be a region in the space spanned by the bare coupling constants where the geometry of spacetime bears some resemblance with the kind of universe we observe around us. That is, the theory should create dynamically an effective background geometry around which there are (small) quantum fluctuations. This is a very nontrivial property of the theory and one we are going to investigate in detail in the present piece of work. New computer simulations presented here confirm in a much more direct way the indirect evidence for such a scenario which we provided earlier in [5,6]. They establish the de Sitter nature of the background spacetime, quantify the fluctuations around it, and set a physical scale for the universes we are dealing with. The main results of our investigation, without the numerical details, were announced in [7] (see also [8]).

The rest of the article is organized as follows. In Sec. II we describe briefly the regularization method of quantum gravity named CDT and the setup of the computer simulations. In Sec. III we present the evidence for an effective background geometry corresponding to the four-dimensional sphere S^4, i.e. Euclidean de Sitter spacetime. Section IV deals with the reconstruction of an effective action for the scale factor of the universe from the computer data, and in Sec. V we analyze the quantum fluctuations around the ''classical'' S^4 solution. Section VI contains an analysis of the geometry of the spatial slices of our computer-generated universe. In Sec. VII we determine the physical sizes of our universes expressed in Planck lengths and try to follow the flow of the gravitational coupling constant of the effective action under a change of the bare coupling constants of the bare classical action used in the path integral. Finally we discuss the results, their interpretation, and future perspectives of the CDT-quantum gravity theory in Sec. VIII.

II. CAUSAL DYNAMICAL TRIANGULATIONS

The approach of causal dynamical triangulations stands in the tradition of [9], which advocated that in a gravitational path integral with the correct Lorentzian signature of spacetime, one should sum over causal geometries only. More specifically, we adopted this idea when it became clear that attempts to formulate a *Euclidean* nonperturbative quantum gravity theory run into trouble in spacetime dimension d larger than 2. At the same time, such a causal reformulation results in a path integral which relates more closely to canonical formulations of quantum gravity.

This implies that we start from Lorentzian simplicial spacetimes with $d = 4$ and insist that only causally well-behaved geometries appear in the (regularized) Lorentzian path integral. A crucial property of our explicit construction is that each of the configurations allows for a rotation to Euclidean signature. We rotate to a Euclidean regime in order to perform the sum over geometries (and rotate back again afterwards if needed). We stress here that although the sum is performed over geometries with Euclidean signature, it is different from what one would obtain in a theory of quantum gravity based *ab initio* on Euclidean spacetimes. The reason is that not all Euclidean geometries with a given topology are included in the ''causal'' sum since, in general, they have no correspondence to a causal Lorentzian geometry.

How do we construct the class of piecewise linear geometries used in the Lorentzian path integral (see [3] for a detailed description)? The most important assumption is the existence of a global proper-time foliation. We assume that the spacetime topology is that of $I \times \Sigma^{(3)}$, where $\Sigma^{(3)}$ denotes an arbitrary three-dimensional manifold. In what follows, we will, for simplicity, study the case of the simplest spatial topology $\Sigma^{(3)} = S^3$, that of a three-sphere. The compactness of S^3 obviates the discussion of spatial boundary conditions for the universe. The spatial geometry at each discrete proper-time step t_n is represented by a triangulation of S^3, made up of equilateral spatial tetrahedra with squared side length $\ell_s^2 \equiv a^2 > 0$. In general, the number $N_3(t_n)$ of tetrahedra and how they are glued together to form a piecewise flat three-dimensional manifold will vary with each time step t_n. In order to obtain a four-dimensional triangulation, the individual three-dimensional slices must still be connected in a causal way, preserving the S^3 topology at all intermediate times

t between t_n and t_{n+1}.[1] This is done by connecting each tetrahedron belonging to the triangulation at time t_n to a vertex belonging to the triangulation at time t_{n+1} by means of a four-simplex which has four timelike links of length squared $\ell_t^2 = -\alpha\ell_s^2$, $\alpha > 0$, interpolating between the adjacent slices [a so-called (4,1)-simplex]. In addition, a triangle in the triangulation at time t_n can be connected to a link in the triangulation at t_{n+1} via a four-simplex with six timelike links [a so-called (3,2)-simplex], again with $\ell_t^2 = -\alpha\ell_s^2$. Conversely, one can connect a link at t_n to a triangle at t_{n+1} to create a (2,3)-simplex and a vertex at t_n to a tetrahedron at t_{n+1} to create a (1,4)-simplex. One can interpolate between subsequent triangulations of S^3 at t_n and t_{n+1} in many distinct ways compatible with the topology $I \times S^3$ of the four-manifold. All these possibilities are summed over in the CDT path integral. The explicit rotation to Euclidean signature is done by performing the rotation $\alpha \to -\alpha$ in the complex lower half-plane, $|\alpha| > 7/12$, such that we have $\ell_t^2 = |\alpha|\ell_s^2$ (see [3] for a discussion).

The Einstein-Hilbert action $S^{\rm EH}$ has a natural geometric implementation on piecewise linear geometries in the form of the Regge action. This is given by the sum of the so-called deficit angles around the two-dimensional "hinges" (subsimplices in the form of triangles), each multiplied by the volume of the corresponding hinge. In view of the fact that we are dealing with piecewise linear and not smooth metrics, there is no unique "approximation" to the usual Einstein-Hilbert action, and one could, in principle, work with a different form of the gravitational action. We will stick with the Regge action, which takes on a very simple form in our case, where the piecewise linear manifold is constructed from just two different types of building blocks. After rotation to Euclidean signature one obtains for the action (see [4] for details)

$$\begin{aligned} S_E^{\rm EH} &= \frac{1}{16\pi^2 G}\int d^4x\sqrt{g}(-R + 2\Lambda) \to S_E^{\rm Regge} \\ &= -(\kappa_0 + 6\Delta)N_0 + \kappa_4(N_4^{(4,1)} + N_4^{(3,2)}) \\ &\quad + \Delta(2N_4^{(4,1)} + N_4^{(3,2)}), \end{aligned} \tag{3}$$

where N_0 denotes the total number of vertices in the four-dimensional triangulation and $N_4^{(4,1)}$ and $N_4^{(3,2)}$ denote the total number of four-simplices described above, i.e. the total number of (4,1)-simplices *plus* (1,4)-simplices and the total number of (3,2)-simplices *plus* (2,3)-simplices, respectively, so that the total number N_4 of four-simplices is $N_4 = N_4^{(4,1)} + N_4^{(3,2)}$. The dimensionless coupling constants κ_0 and κ_4 are related to the bare gravitational and bare cosmological coupling constants, with appropriate powers of the lattice spacing a already absorbed into κ_0 and κ_4. The *asymmetry parameter* Δ is related to the parameter α introduced above, which describes the relative scale between the (squared) lengths of spacelike and timelike links. It is both convenient and natural to keep track of this parameter in our setup, which from the outset is not isotropic in time and space directions; see again [4] for a detailed discussion. Since we will, in the following, work with the path integral after Wick rotation, let us redefine $\tilde{\alpha} := -\alpha$ [4], which is positive in the Euclidean domain.[2] For future reference, the Euclidean four-volume of our universe for a given choice of $\tilde{\alpha}$ is given by

$$V_4 = C_4 a^4\left(\frac{\sqrt{8\tilde{\alpha} - 3}}{\sqrt{5}}N_4^{(4,1)} + \frac{\sqrt{12\tilde{\alpha} - 7}}{\sqrt{5}}N_4^{(3,2)}\right), \tag{4}$$

where $C_4 = \sqrt{5}/96$ is the four-volume of an equilateral four-simplex with edge length $a = 1$ (see [3] for details). It is convenient to rewrite expression (4) as

$$V_4 = \tilde{C}_4(\xi)a^4 N_4^{(4,1)} = \tilde{C}_4(\xi)a^4 N_4/(1 + \xi), \tag{5}$$

where ξ is the ratio

$$\xi = N_4^{(3,2)}/N_4^{(4,1)}, \tag{6}$$

and $\tilde{C}_4(\xi)a^4$ is a measure of the "effective four-volume" of an "average" four-simplex. In computing (3), we have assumed that the spacetime manifold is compact without boundaries; otherwise, appropriate boundary terms must be added to the action.

The path integral or partition function for the CDT version of quantum gravity is now

$$\begin{aligned} Z(G, \Lambda) &= \int \mathcal{D}[g]\mathrm{e}^{-S_E^{\rm EH}[g]} \to Z(\kappa_0, \kappa_4, \Delta) \\ &= \sum_{\mathcal{T}} \frac{1}{C_{\mathcal{T}}}\mathrm{e}^{-S_E(\mathcal{T})}, \end{aligned} \tag{7}$$

where the summation is over all causal triangulations $\mathcal{T}$ of the kind described above, and we have dropped the superscript "Regge" on the discretized action. The factor $1/C_{\mathcal{T}}$ is a symmetry factor, given by the order of the automorphism group of the triangulation $\mathcal{T}$. The actual setup for the simulations is as follows. We choose a fixed number N of spatial slices at proper times t_1, $t_2 = t_1 + a_t$, up to $t_N = t_1 + (N - 1)a_t$, where $\Delta t \equiv a_t$ is the discrete lattice spacing in the temporal direction and $T = Na_t$ the total extension of the universe in proper time. For convenience we identify t_{N+1} with t_1, in this way imposing the topology $S^1 \times S^3$ rather than $I \times S^3$. This choice does not affect physical results, as will become clear in due course.

[1] This implies the absence of branching of the spatial universe into several disconnected pieces, so-called *baby universes*, which (in Lorentzian signature) would inevitably be associated with causality violations in the form of degeneracies in the light cone structure, as has been discussed elsewhere (see, for example, [10]).

[2] The most symmetric choice is $\tilde{\alpha} = 1$, corresponding to vanishing asymmetry, $\Delta = 0$.

Our next task is to *evaluate* the nonperturbative sum in (7), if possible, analytically. Although this can be done in spacetime dimension $d = 2$ ([11], and see [12] for recent developments) and at least partially in $d = 3$ [13,14], an analytic solution in four dimensions is currently out of reach. However, we are in the fortunate situation that $Z(\kappa_0, \kappa_4, \Delta)$ can be studied quantitatively with the help of Monte Carlo simulations. The type of algorithm needed to update the piecewise linear geometries has been around for a while, starting from the use of dynamical triangulations in bosonic string theory (two-dimensional Euclidean triangulations) [15–17], and was later extended to their application in Euclidean four-dimensional quantum gravity [18,19]. In [3] the algorithm was modified to accommodate the geometries of the CDT setup. Note that the algorithm is such that it takes the symmetry factor $C_{\mathcal{T}}$ into account automatically.

We have performed extensive Monte Carlo simulations of the partition function Z for a number of values of the bare coupling constants. As reported in [4], there are regions of the coupling constant space which do not appear relevant for continuum physics in that they seem to suffer from problems similar to the ones found earlier in *Euclidean* quantum gravity constructed in terms of dynamical triangulations, which essentially led to its abandonment in $d > 2$. Namely, when the (inverse, bare) gravitational coupling κ_0 is sufficiently large, the Monte Carlo simulations exhibit a sequence in time direction of small, disconnected universes, none of them showing any sign of the scaling one would expect from a macroscopic universe. We believe that this phase of the system is a Lorentzian version of the branched-polymer phase of Euclidean quantum gravity. By contrast, when Δ is sufficiently small the simulations reveal a universe with a vanishing temporal extension of only a few lattice spacings, ending both in the past and the future in a vertex of very high order, connected to a large fraction of all vertices. This phase is most likely related to the so-called crumpled phase of Euclidean quantum gravity. The crucial and new feature of the quantum superposition in terms of *causal* dynamical triangulations is the appearance of a region in coupling constant space which is different and interesting and where continuum physics may emerge. It is in this region that we have performed the simulations reported in this article, and where previous work has already uncovered a number of intriguing physical results [4–6,20].

In the Euclideanized setting the value of the cosmological constant determines the spacetime volume V_4 since the two appear in the action as conjugate variables. We therefore have $\langle V_4 \rangle \sim G/\Lambda$ in a continuum notation, where G is the gravitational coupling constant and Λ the cosmological constant. In computer simulations it is more convenient to keep the four-volume fixed or partially fixed. We will implement this by fixing the total number of four-simplices of type $N_4^{(4,1)}$ or, equivalently, the total number N_3 of tetrahedra making up the spatial S^3 triangulations at times t_i, $i = 1, \ldots, N$,

$$N_3 = \sum_{i=1}^{N} N_3(t_i) = \frac{1}{2} N_4^{(4,1)}. \tag{8}$$

We know from the simulations that in the phase of interest $\langle N_4^{(4,1)} \rangle \propto \langle N_4^{(3,2)} \rangle$ as the total volume is varied [4]. This effectively implies that we only have two bare coupling constants κ_0, Δ in (7), while we compensate by hand for the coupling constant κ_4 by studying the partition function $Z(\kappa_0, \Delta; N_4^{(4,1)})$ for various $N_4^{(4,1)}$. To keep track of the ratio $\xi(\kappa_0, \Delta)$ between the expectation value $\langle N_4^{(3,2)} \rangle$ and $N_4^{(4,1)}$, which depends weakly on the coupling constants, we write [cf. Eq. (6)]

$$\langle N_4 \rangle = N_4^{(4,1)} + \langle N_4^{(3,2)} \rangle = N_4^{(4,1)}(1 + \xi(\kappa_0, \Delta)). \tag{9}$$

For all practical purposes we can regard N_4 in a Monte Carlo simulation as fixed. The relation between the partition function we use and the partition function with variable four-volume is given by the Laplace transformation

$$Z(\kappa_0, \kappa_4, \Delta) = \int_0^\infty \mathrm{d}N_4 \mathrm{e}^{-\kappa_4 N_4} Z(\kappa_0, N_4, \Delta), \tag{10}$$

where, strictly speaking, the integration over N_4 should be replaced by a summation over the discrete values that N_4 can take.

III. THE MACROSCOPIC DE SITTER UNIVERSE

The Monte Carlo simulations referred to above will generate a sequence of spacetime histories. An individual spacetime history is not an observable, in the same way as a path $x(t)$ of a particle in the quantum-mechanical path integral is not. However, it is perfectly legitimate to talk about the *expectation value* $\langle x(t) \rangle$ as well as the *fluctuations around* $\langle x(t) \rangle$. Both of these quantities are, in principle, calculable in quantum mechanics.

Obviously, there are many more dynamical variables in quantum gravity than there are in the particle case. We can still imitate the quantum-mechanical situation by picking out a particular one, for example, the spatial three-volume $V_3(t)$ at proper time t. We can measure its expectation value $\langle V_3(t) \rangle$ as well as fluctuations around it. The former gives us information about the large-scale "shape" of the universe we have created in the computer. In this section, we will describe the measurements of $\langle V_3(t) \rangle$, keeping a more detailed discussion of the fluctuations to Sec. V below.

A "measurement" of $V_3(t)$ consists of a table $N_3(i)$, where $i = 1, \ldots, N$ denotes the number of time slices. Recall from Sec. II that the sum over slices $\sum_{i=1}^{N} N_3(i)$ is kept constant. The time axis has a total length of N time

steps, where $N = 80$ in the actual simulations, and we have cyclically identified time slice $N + 1$ with time slice 1.

What we observe in the simulations is that for the range of discrete volumes N_4 under study, the universe does *not* extend (i.e. has appreciable three-volume) over the entire time axis, but rather is localized in a region much shorter than 80 time slices. Outside this region the spatial extension $N_3(i)$ will be minimal, consisting of the minimal number (five) of tetrahedra needed to form a three-sphere S^3, plus occasionally a few more tetrahedra.[3] This thin "stalk" therefore carries little four-volume, and in a given simulation we can, for most practical purposes, consider the total four-volume of the remainder, the extended universe, as fixed.

In order to perform a meaningful average over geometries which explicitly refers to the extended part of the universe, we have to remove the translational zero mode which is present. During the Monte Carlo simulations the extended universe will fluctuate in shape and its *center of mass* (or, more to the point, its *center of volume*) will perform a slow random walk along the time axis. Since we are dealing with a circle (the compactified time axis), the center of volume is not uniquely defined (it is clearly arbitrary for a constant volume distribution), and we must first define what we mean by such a concept. Here we take advantage of the empirical fact that our dynamically generated universes decompose into an extended piece and a stalk, with the latter containing less than one percent of the total volume. We are clearly interested in a definition such that the center of volume of a given configuration lies in the center of the extended region. One also expects that any sensible definition will be unique up to contributions related to the stalk and to the discreteness of the time steps. In total this amounts to an ambiguity of the center of volume of one lattice step in the time direction.

In analyzing the computer data we have chosen one specific definition which is in accordance with the discussion above.[4] Maybe surprisingly, it turns out that the inherent ambiguity in the choice of a definition of the center of volume—even if it is only of the order of one lattice spacing—will play a role later on in our analysis of the quantum fluctuations. For each universe used in the measurements (a "path" in the gravitational path integral) we will denote the center-of-volume time coordinate calculated by our algorithm by $i_{\rm cv}$. From now on, when comparing different universes, i.e. when performing ensemble averages, we will redefine the temporal coordinates according to

$$N_3^{\rm new}(i) = N_3(1 + \mathrm{mod}(i + i_{\rm cv} - 1, N)), \qquad (11)$$

such that the center of volume is located at 0.

Having defined in this manner the center of volume along the time direction of our spacetime configurations, we can now perform superpositions of such configurations and define the average $\langle N_3(i)\rangle$ as a function of the discrete time i. The results of measuring the average discrete spatial size of the universe at various discrete times i are illustrated in Fig. 1 and can be succinctly summarized by the formula

$$N_3^{cl}(i) := \langle N_3(i)\rangle = \frac{N_4}{2(1+\xi)}\,\frac{3}{4}\,\frac{1}{s_0 N_4^{1/4}}\cos^3\!\left(\frac{i}{s_0 N_4^{1/4}}\right),$$
$$s_0 \approx 0.59, \qquad (12)$$

where $N_3(i)$ denotes the number of three-simplices in the spatial slice at discretized time i, and N_4 the total number of four-simplices in the entire universe. Since we are keeping $N_4^{(4,1)}$ fixed in the simulations and since ξ changes with the choice of bare coupling constants, it is sometimes convenient to rewrite (12) as

$$N_3^{cl}(i) = \frac{1}{2}N_4^{(4,1)}\,\frac{3}{4}\,\frac{1}{\tilde{s}_0 (N_4^{(4,1)})^{1/4}}\cos^3\!\left(\frac{i}{\tilde{s}_0 (N_4^{(4,1)})^{1/4}}\right), \qquad (13)$$

where $\tilde{s}_0$ is defined by $\tilde{s}_0 (N_4^{(4,1)})^{1/4} = s_0 N_4^{1/4}$. Of course, formula (12) is only valid in the extended part of the

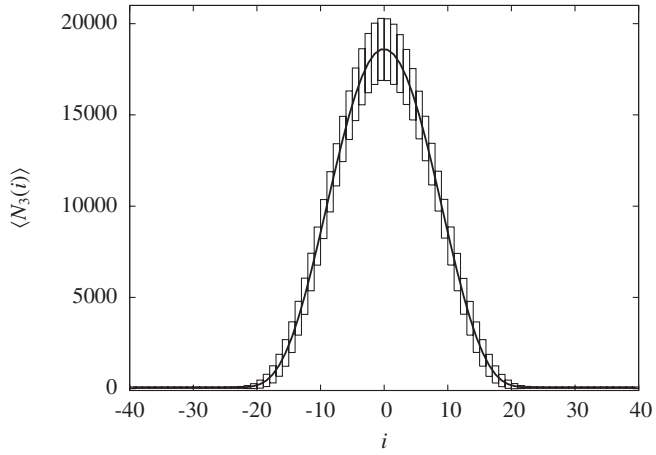

FIG. 1. Background geometry $\langle N_3(i)\rangle$: Monte Carlo measurements for fixed $N_4^{(4,1)} = 160.000$ ($N_4 = 362.000$) and best fit (12) yield indistinguishable curves at given plot resolution. The bars indicate the average size of quantum fluctuations.

[3]This kinematical constraint ensures that the triangulation remains a *simplicial manifold* in which, for example, two d-simplices are not allowed to have more than one $(d-1)$-simplex in common.

[4]Explicitly, we consider the quantity

$$\mathrm{CV}(i') = \left|\sum_{i=-N/2}^{N/2-1} (i + 0.5) N_3(1 + \mathrm{mod}(i' + i - 1, N))\right|$$

where $\mathrm{mod}(i, N)$ is defined as the remainder, on division of i by N, and find the value of $i' \in \{1, \ldots, N\}$ for which $\mathrm{CV}(i')$ is smallest. We denote this i' by $i_{\rm cv}$. If there is more than one minimum, we choose the value which has the largest three-volume $N_3(i')$. Let us stress that this is just one of many definitions of $i_{\rm cv}$. All other sensible definitions will, for the type of configurations considered here, agree to within one lattice spacing.

universe where the spatial three-volumes are larger than the minimal cutoff size.

The data shown in Fig. 1 have been collected at the particular values $(\kappa_0, \Delta) = (2.2, 0.6)$ of the bare coupling constants and for $N_4 = 362.000$ (corresponding to $N_4^{(4,1)} = 160.000$). For these values of (κ_0, Δ) we have verified relation (12) for N_4 ranging from 45.500 to 362.000 building blocks (45.500, 91.000, 181.000, and 362.000). After rescaling the time and volume variables by suitable powers of N_4 according to relation (12), and plotting them in the same way as in Fig. 1, one finds almost total agreement between the curves for different spacetime volumes.[5] Equation (12) shows that spatial volumes scale according to $N_4^{3/4}$ and time intervals according to $N_4^{1/4}$, as one would expect for a genuinely *four*-dimensional spacetime. This strongly suggests a translation of (12) to a continuum notation. The most natural identification is given by

$$\sqrt{g_{tt}} V_3^{cl}(t) = V_4 \frac{3}{4B} \cos^3\left(\frac{t}{B}\right), \tag{14}$$

where we have made the identifications

$$\frac{t_i}{B} = \frac{i}{s_0 N_4^{1/4}}, \qquad \Delta t_i \sqrt{g_{tt}} V_3(t_i) = 2\tilde{C}_4 N_3(i) a^4, \tag{15}$$

such that we have

$$\int dt \sqrt{g_{tt}} V_3(t) = V_4. \tag{16}$$

In (15), $\sqrt{g_{tt}}$ is the constant proportionality factor between the time t and genuine continuum proper time τ, $\tau = \sqrt{g_{tt}} t$. (The combination $\Delta t_i \sqrt{g_{tt}} V_3$ contains $\tilde{C}_4$, related to the four-volume of a four-simplex rather than the three-volume corresponding to a tetrahedron, because its time integral must equal V_4). Writing $V_4 = 8\pi^2 R^4/3$, and $\sqrt{g_{tt}} = R/B$, Eq. (14) is seen to describe a Euclidean *de Sitter universe* (a four-sphere, the maximally symmetric space for a positive cosmological constant) as our searched-for, dynamically generated background geometry. In the parametrization of (14) this is the classical solution to the action

$$S = \frac{1}{24\pi G} \int dt \sqrt{g_{tt}} \left(\frac{g^{tt} \dot{V}_3^2(t)}{V_3(t)} + k_2 V_3^{1/3}(t) - \lambda V_3(t) \right), \tag{17}$$

where $k_2 = 9(2\pi^2)^{2/3}$ and λ is a Lagrange multiplier, fixed by requiring that the total four-volume be V_4, $\int dt \sqrt{g_{tt}} V_3(t) = V_4$. Up to an overall sign, this is precisely the Einstein-Hilbert action for the scale factor $a(t)$ of a homogeneous, isotropic universe [rewritten in terms of the spatial three-volume $V_3(t) = 2\pi^2 a(t)^3$], although we of course never put any such simplifying symmetry assumptions into the CDT model.

For a fixed, finite four-volume V_4 and when applying scaling arguments, it can be convenient to rewrite (17) in terms of dimensionless units by introducing $s = t/V_4^{1/4}$ and $V_3(t) = V_4^{3/4} v_3(s)$, in which case (17) becomes

$$S = \frac{1}{24\pi} \frac{\sqrt{V_4}}{G} \int ds \sqrt{g_{ss}} \left(\frac{g^{ss} \dot{v}_3^2(s)}{v_3(s)} + k_2 v_3^{1/3}(s) \right), \tag{18}$$

now assuming that $\int ds \sqrt{g_{ss}} v_3(s) = 1$, and with $g_{ss} \equiv g_{tt}$. A discretized, dimensionless version of (17) is

$$S_{\text{discr}} = k_1 \sum_i \left(\frac{(N_3(i+1) - N_3(i))^2}{N_3(i)} + \tilde{k}_2 N_3^{1/3}(i) \right), \tag{19}$$

where $\tilde{k}_2 \propto k_2$. This can be seen by applying the scaling (12), namely, $N_3(i) = N_4^{3/4} n_3(s_i)$ and $s_i = i/N_4^{1/4}$. With this scaling, the action (19) becomes

$$S_{\text{discr}} = k_1 \sqrt{N_4} \sum_i \Delta s \left(\frac{1}{n_3(s_i)} \left(\frac{n_3(s_{i+1}) - n_3(s_i)}{\Delta s} \right)^2 + \tilde{k}_2 n_3^{1/3}(s_i) \right), \tag{20}$$

where $\Delta s = 1/N^{1/4}$, and therefore has the same form as (18). This enables us to finally conclude that the identifications (15) when used in the action (19) lead naïvely to the continuum expression (17) under the identification

$$G = \frac{a^2}{k_1} \frac{\sqrt{\tilde{C}_4} \tilde{s}_0^2}{3\sqrt{6}}. \tag{21}$$

In more detail, comparing the kinetic terms in (17) and (19),

$$\frac{1}{24\pi G} \sum_i \frac{(V_3(t_i + \Delta t_i) - V_3(t_i))^2}{\Delta t_i \sqrt{g_{t_i t_i}} V_3(t_i)} = k_1 \sum_i \frac{(N_3(i+1) - N_3(i))^2}{N_3(i)}, \tag{22}$$

and using Eq. (15) leads to

$$G = \frac{a^4}{k_1} \frac{2\sqrt{\tilde{C}_4}}{24\pi g_{t_i t_i} (\Delta t_i)^2}. \tag{23}$$

Equation (21) now follows from the equations

$$(\Delta t_i)^2 = \frac{B^2}{s_0^2 \sqrt{N_4}}, \qquad \tilde{s}_0^2 = s_0^2 \sqrt{1 + \xi}, \tag{24}$$

$$V_4 = \frac{8\pi^2}{3} R^4 = \frac{\tilde{C}_4}{1 + \xi} N_4 a^4, \qquad g_{t_i t_i} = \frac{R^2}{B^2}. \tag{25}$$

Next, let us comment on the universality of these results. First, we have checked that they are not dependent on the particular definition of time slicing we have been using, in

[5] By contrast, the quantum fluctuations indicated in Fig. 1 as vertical bars *are* volume dependent and will become larger as the total four-volume becomes smaller; see Sec. V below for details.

the following sense. By construction of the piecewise linear CDT geometries, we have at each integer time step $t_i = ia_t$ a spatial surface consisting of $N_3(i)$ tetrahedra. Alternatively, one can choose as reference slices for the measurements of the spatial volume noninteger values of time, for example, all time slices at discrete times $i - 1/2$, $i = 1, 2, \ldots$. In this case the "triangulation" of the spatial three-spheres consists of tetrahedra—from cutting a (4,1)- or a (1,4)-simplex halfway—and "boxes," obtained by cutting a (2,3)- or (3,2)-simplex (the geometry of this is worked out in [21]). We again find a relation like (12) if we use the total number of spatial building blocks in the intermediate slices (tetrahedra + boxes) instead of just the tetrahedra.

Second, we have repeated the measurements for other values of the bare coupling constants. As long as we stay in the phase where an extended universe is observed (called "phase C" in Ref. [4]), a relation like (12) remains valid. In addition, the value of s_0, defined in Eq. (12), is almost unchanged until we get close to the phase transition lines beyond which the extended universe disappears. Figure 2 shows the average shape $\langle N_3(t)\rangle$ for $\Delta = 0.6$ and for κ_0 equal to 2.2 and 3.6. Only for the values of κ_0 around 3.6 and larger will the measured $\langle N_3(t)\rangle$ differ significantly from the value at 2.2. For values larger than 3.8 (at $\Delta = 0.6$), the universe will disintegrate into a number of small and disconnected components distributed randomly along the time axis, and one can no longer fit the distribution $\langle N_3(t)\rangle$ to the formula (12). Figure 3 shows the average shape $\langle N_3(t)\rangle$ for $\kappa_0 = 2.2$ and Δ equal to 0.2 and 0.6. Here the value $\Delta = 0.2$ is close to the phase transition where the extended universe will flatten out to a universe with a time extension of a few lattice spacings only. Later we will show that while s_0 is almost unchanged, the constant k_1 in (19), which governs the quantum fluctuations around the mean value $\langle N_3(t)\rangle$, is more sensitive to a change of the bare coupling constants, in particular in the case where we change κ_0 (while leaving Δ fixed).

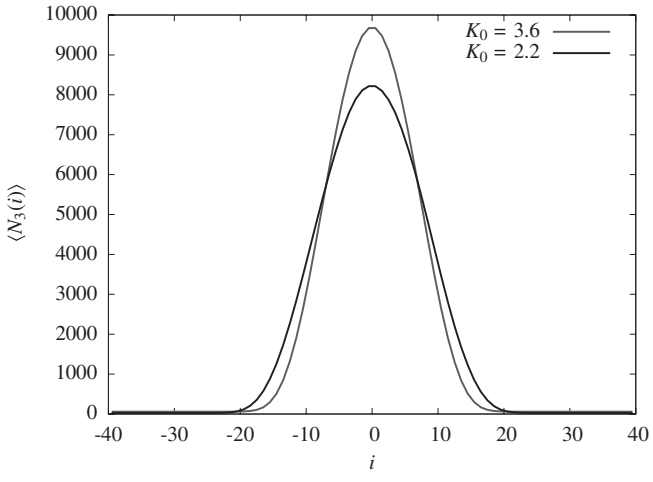

FIG. 2. The measured average shape $\langle N_3(i)\rangle$ of the quantum universe at $\Delta = 0.6$, for $\kappa_0 = 2.2$ (broader distribution) and $\kappa_0 = 3.6$ (narrower distribution), taken at $N_4^{(4,1)} = 160.000$.

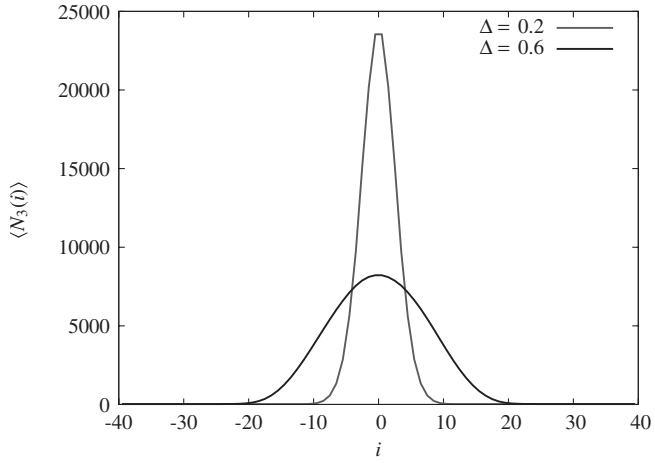

FIG. 3. The measured average shape $\langle N_3(i)\rangle$ of the quantum universe at $\kappa_0 = 2.2$, for $\Delta = 0.6$ (broad distribution) and $\Delta = 0.2$ (narrow distribution), both taken at $N_4^{(4,1)} = 160.000$.

IV. CONSTRUCTIVE EVIDENCE FOR THE EFFECTIVE ACTION

While the functional form (12) for the three-volume fits the data perfectly and the corresponding continuum effective action (17) reproduces the continuum version (14) of (12), it is still of interest to check to what extent one can reconstruct the discretized version (19) of the continuum action (17) from the data explicitly. Stated differently, we would like to understand whether there are other effective actions which reproduce the data equally well. As we will demonstrate by explicit construction in this section, there is good evidence for the uniqueness of the action (19).

The data we have are twofold: the measurement of $N_3(i)$, that is, the three-volume at the discrete time step i, and the measurement of the three-volume correlator $N_3(i)N_3(j)$. Having created K statistically independent configurations $N_3^{(k)}(i)$ by Monte Carlo simulation allows us to construct the average

$$\bar{N}_3(i) := \langle N_3(i)\rangle \cong \frac{1}{K}\sum_k N_3^{(k)}(i), \tag{26}$$

where the superscript in $(\cdot)^{(k)}$ denotes the result of the kth configuration sampled, as well as the covariance matrix

$$C(i,j) \cong \frac{1}{K}\sum_k (N_3^{(k)}(i) - \bar{N}_3(i))(N_3^{(k)}(j) - \bar{N}_3(j)). \tag{27}$$

Since we have fixed the sum $\sum_{i=1}^N N_3(i)$ (recall that N denotes the fixed number of time steps in a given simulation), the covariance matrix has a zero mode, namely, the constant vector $e_i^{(0)}$,

$$\sum_j C(i,j)e_j^{(0)} = 0, \qquad e_i^{(0)} = 1/\sqrt{N} \quad \forall\ i. \tag{28}$$

A spectral decomposition of the symmetric covariance matrix gives

$$\hat{C} = \sum_{a=1}^{N-1} \lambda_a |e^{(a)}\rangle\langle e^{(a)}|, \tag{29}$$

where we assume the $N-1$ other eigenvalues of the covariance matrix $\hat{C}_{ij}$ are different from zero. We now define the "propagator" $\hat{P}$ as the inverse of $\hat{C}$ on the subspace orthogonal to the zero mode $e^{(0)}$, that is,

$$\begin{aligned} \hat{P} &= \sum_{a=1}^{N-1} \frac{1}{\lambda_a} |e^{(a)}\rangle\langle e^{(a)}| = (\hat{C} + \hat{A})^{-1} - \hat{A}, \\ \hat{A} &= |e^{(0)}\rangle\langle e^{(0)}|. \end{aligned} \tag{30}$$

We now assume we have a discretized action which can be expanded around the expectation value $\bar{N}_3(i)$ according to

$$S_{\mathrm{discr}}[\bar{N}+n] = S_{\mathrm{discr}}[\bar{N}] + \frac{1}{2}\sum_{i,j} n_i \hat{P}_{ij} n_j + O(n^3). \tag{31}$$

If the quadratic approximation describes the quantum fluctuations around the expectation value $\bar{N}$ well, the inverse of $\hat{P}$ will be a good approximation to the covariance matrix. Conversely, still assuming the quadratic approximation gives a good description of the fluctuations, the $\hat{P}$ constructed from the covariance matrix will, to a good approximation, allow us to reconstruct the action via (31).

Simply by looking at the inverse $\hat{P}$ of the measured covariance matrix, defined as described above, we observe that it is, to a very good approximation, small and constant except on the diagonal and the entries neighboring the diagonal. We can then decompose it into a "kinetic" and a "potential" term. The kinetic part $\hat{P}^{\mathrm{kin}}$ is defined as the matrix with nonzero elements on the diagonal and in the neighboring entries, such that the sum of the elements in a row or a column is always zero,

$$\hat{P}^{\,\mathrm{kin}} = \sum_{i=1}^{N} p_i \hat{X}^{(i)}, \tag{32}$$

where the matrix $\hat{X}^{(i)}$ is given by

$$\hat{X}^{\,(i)}_{jk} = \delta_{ij}\delta_{ik} + \delta_{(i+1)j}\delta_{(i+1)k} - \delta_{(i+1)j}\delta_{ik} - \delta_{ij}\delta_{(i+1)k}. \tag{33}$$

Note that the range of $\hat{P}^{\mathrm{kin}}$ lies by definition in the subspace orthogonal to the zero mode. Similarly, we define the potential term as the projection of a diagonal matrix $\hat{D}$ on the subspace orthogonal to the zero mode

$$\hat{P}^{\,\mathrm{pot}} = (\hat{I} - \hat{A})\hat{D}(\hat{I} - \hat{A}) = \sum_{i=1}^{N} u_i \hat{Y}^{(i)}. \tag{34}$$

The diagonal matrix $\hat{D}$ and the matrices $\hat{Y}^{(i)}$ are defined by

$$\hat{D}_{\,jk} = u_j \delta_{jk}, \qquad \hat{Y}^{(i)}_{jk} = \delta_{ij}\delta_{ik} - \frac{\delta_{ij} + \delta_{ik}}{N} + \frac{1}{N^2}, \tag{35}$$

and $\hat{I}$ denotes the $N \times N$ unit matrix.

The matrix $\hat{P}$ is obtained from the numerical data by inverting the covariance matrix $\hat{C}$ after subtracting the zero mode, as described above. We can now try to find the best values of the p_i's and u_i's by a least-χ^2 fit[6] to

$$\mathrm{tr}\,(\hat{P} - (\hat{P}^{\mathrm{kin}} + \hat{P}^{\mathrm{pot}}))^2. \tag{36}$$

Let us look at the discretized minisuperspace action (19) which obviously has served as an inspiration for the definitions of $\hat{P}^{\mathrm{kin}}$ and $\hat{P}^{\mathrm{pot}}$. Expanding $N_3(i)$ to second order around $\bar{N}_3(i)$, one obtains the identifications

$$\bar{N}_{\,3}(i) = \frac{2k_1}{p_i}, \qquad U''(\bar{N}_3(i)) = -u_i, \tag{37}$$

where $U(N_3(i)) = k_1\tilde{k}_2 N_3^{1/3}(i)$ denotes the potential term in (19). We use the fitted coefficients p_i to reconstruct $\bar{N}_3(i)$ and then compare these reconstructed values with the averages $\bar{N}_3(i)$ measured directly. Similarly, we can use the measured u_i's to reconstruct the second derivatives $U''(\bar{N}_3(i))$ and compare them to the form $\bar{N}_3^{-5/3}(i)$ coming from (19).

The reconstruction of $\bar{N}_3(i)$ is illustrated in Fig. 4 for a variety of four-volumes N_4 and compared with the directly measured expectation values $\bar{N}_3(i)$. It is seen that the reconstruction works very well and, *most importantly*, the coupling constant k_1, which in this way is determined independently for each four-volume N_4, really *is* independent of N_4 in the range of N_4's considered, as it should be.

We will now try to extract the potential $U''(\bar{N}_3(i))$ from the information contained in the matrix $\hat{P}^{\mathrm{pot}}$. The determination of $U''(\bar{N}_3(i))$ is not an easy task as can be understood from Fig. 5, which shows the measured coefficients u_i extracted from the matrix $\hat{P}^{\mathrm{pot}}$, and which we consider somewhat remarkable. The interpolated curve makes an abrupt jump by 2 orders of magnitude going from the extended part of the universe (stretching over roughly 40

[6] A χ^2 fit of the form (36) gives the same weight to each three-volume $N_3(i)$. One might argue that more weight should be given to the larger $N_3(i)$ in a configuration since we are interested in the continuum physics and not in what happens in the stalk where $N_3(i)$ is very small. We have tried various χ^2 fits with reasonable weights associated with the three-volumes $N_3(i)$. The kinetic term, which is the dominant term, is insensitive to any (reasonable) weight associated with $N_3(i)$. The potential term, which will be analyzed below, is more sensitive to the choice of the weight. However, the general power law dependence reported below is again unaffected by this choice.

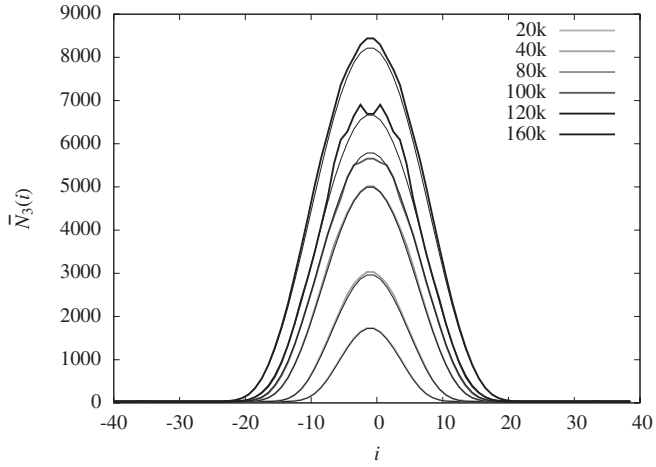

FIG. 4. The directly measured expectation values $\bar{N}_3(i)$ (thick gray curves), compared to the averages $\bar{N}_3(i)$ reconstructed from the measured covariance matrix $\hat{C}$ (thin black curves), for $\kappa_0 = 2.2$ and $\Delta = 0.6$, at various fixed volumes $N_4^{(4,1)}$. The twofold symmetry of the interpolated curves around the central symmetry axis results from an explicit symmetrization of the collected data.

time steps) to the stalk. The occurrence of this jump is entirely dynamical; no distinction has ever been made by hand between the stalk and the bulk.

There are at least two reasons for why it is difficult to determine the potential numerically. First, the results are ''contaminated'' by the presence of the stalk. Since it is of cutoff size, its dynamics is dominated by fluctuations which likewise are of cutoff size. They will take the form of short-time subdominant contributions in the correlator matrix $\hat{C}$. Unfortunately, when we invert $\hat{C}$ to obtain the propagator $\hat{P}$, the same excitations will correspond to the largest eigenvalues and give a very large contribution.

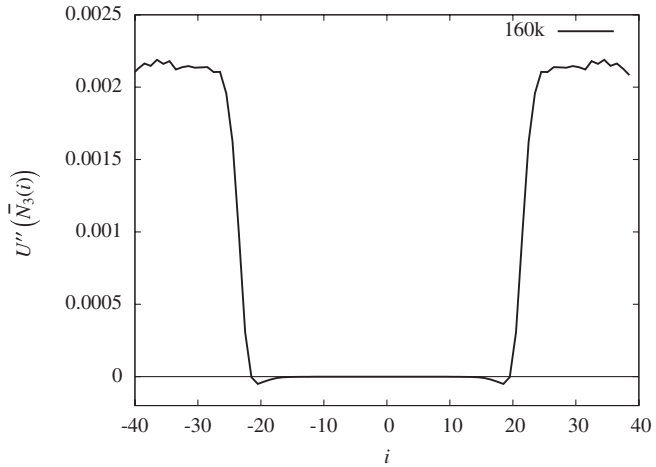

FIG. 5. Reconstruction of the second derivative $U''(\bar{N}_3(i))$ from the coefficients u_i, for $\kappa_0 = 2.2$ and $\Delta = 0.6$ and $N_4^{(4,1)} = 160.000$.

Although the stalk contribution in the matrix $\hat{C}$ is located away from the bulk-diagonal, it can be seen from the appearance of the $1/N^2$-term in Eqs. (34) and (35) that after the projection orthogonal to the zero mode the contributions from the stalk will also affect the remainder of the geometry in the form of fluctuations around a small constant value. In deriving Fig. 6 we have subtracted this constant value as best as possible. However, the *fluctuations* of the stalk cannot be subtracted, and only good statistics can eventually eliminate their effect on the behavior of the extended part of the quantum universe. The second (and less serious) reason is that from a numerical point of view the potential term is always subdominant to the kinetic term for the individual spacetime histories in the path integral. For instance, consider the simple example of the harmonic oscillator. Its discretized action reads

$$S = \sum_{i=1}^{N} \Delta t \left[\left(\frac{x_{i+1} - x_i}{\Delta t} \right)^2 + \omega^2 x_i^2 \right], \tag{38}$$

from which we deduce that the ratio between the kinetic and potential terms will be of order $1/\Delta t$ as Δt tends to zero. This reflects the well-known fact that the kinetic term will dominate and go to infinity in the limit as $\Delta t \to 0$, with a typical path being nowhere differentiable. The same will be true when dealing with a more general action like (17) and its discretized version (19), where Δt scales like $\Delta t \sim 1/N_4^{1/4}$. Of course, a *classical* solution will behave differently: there the kinetic term will be comparable to the potential term. However, when extracting the potential term directly from the data, as we are doing, one is confronted with this issue.

The range of the discrete three-volumes $N_3(i)$ in the extended universe is from several thousand down to 5, the kinematically allowed minimum. However, the behavior for the very small values of $N_3(i)$ near the edge of the extended universe is likely to be mixed in with discretiza-

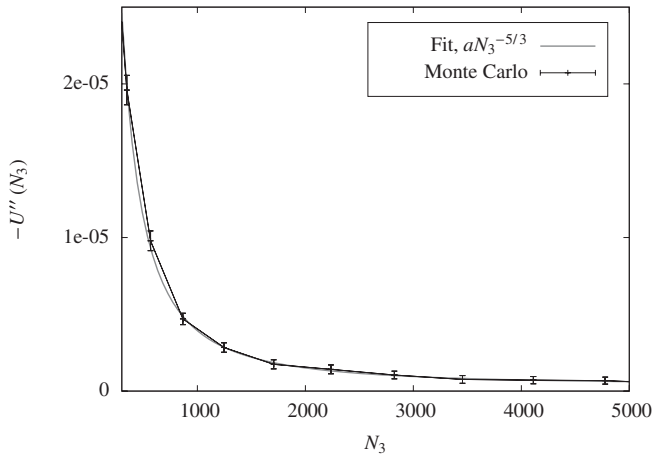

FIG. 6. The second derivative $-U''(N_3)$ as measured for $N_4^{(4,1)} = 160.000$ and $\kappa_0 = 2.2$ and $\Delta = 0.6$.

tion effects. In order to test whether one really has a $N_3^{1/3}(i)$-term in the action, one should therefore only use values of $N_3(i)$ somewhat larger than 5. This has been done in Fig. 6, where we have converted the coefficients u_i from functions of the discrete time steps i into functions of the background spatial three-volume $\bar{N}_3(i)$ using the identification in (37) (the conversion factor can be read off the relevant curve in Fig. 4). It should be emphasized that Fig. 6 is based on data from the extended part of the spacetime only; the variation comes entirely from the central region between times -20 and 20 in Fig. 5, which explains why it has been numerically demanding to extract a good signal. The data presented in Fig. 6 were taken at a discrete volume $N_4^{(4,1)} = 160.000$, and fit the form $N_3^{-5/3}$ well, corresponding to a potential $\tilde{k}_2 N_3^{1/3}$. There is a very small residual constant term present in this fit, which presumably is due to the projection onto the space orthogonal to the zero mode, as already discussed earlier. In view of the fact that its value is quite close to the noise level with our present statistics, we have simply chosen to ignore it in the remaining discussion.

Apart from obtaining the correct power $N_3^{-5/3}$ for the potential for a given spacetime volume N_4, it is equally important that the coefficient in front of this term be independent of N_4. This seems to be the case, as is shown in Fig. 7, where we have plotted the measured potentials in terms of reduced, dimensionless variables which make the comparison between measurements for different N_4's easier.—In summary, we conclude that the data allow us to reconstruct the action (19) with good precision.

Let us emphasize a remarkable aspect of this result. Our starting point was the Regge action for CDT, as described

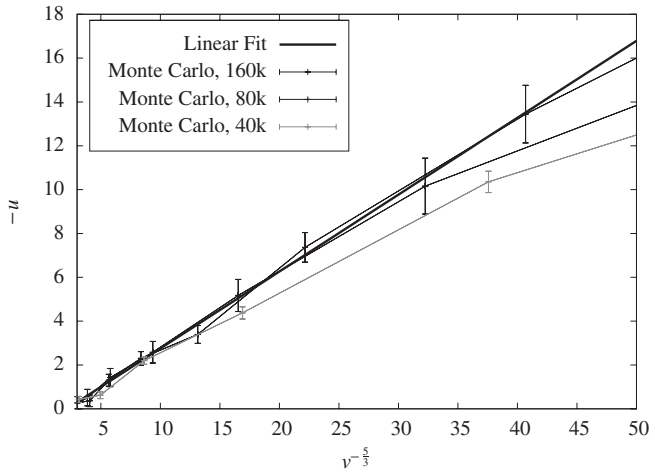

FIG. 7. The dimensionless second derivative $u = N_4^{5/4} U''(N_3)$ plotted against $\nu^{-5/3}$, where $\nu = N_3/N_4^{3/4}$ is the dimensionless spatial volume, for $N_4^{(4,1)} = 40.000$, 80.000, and 160.000, $\kappa_0 = 2.2$ and $\Delta = 0.6$. One expects a universal straight line near the origin (i.e. for large volumes) if the power law $U(N_3) \propto N^{1/3}$ is correct.

in Sec. II above. However, the effective action we have generated dynamically by performing the nonperturbative sum over histories is only indirectly related to this "bare" action. Likewise, the coupling constant k_1 which appears in front of the effective action, and which we view as related to the gravitational coupling constant G by Eq. (21), has no obvious direct relation to the bare coupling κ_0 appearing in the Regge action (3) and in (7). Nevertheless, the leading terms in the effective action for the scale factor are precisely the ones presented in (19). That a kinetic term with a second-order derivative appears as a leading term in an effective action is maybe less surprising, but it is remarkable and very encouraging for the entire CDT-quantization program that the kinetic term appears in precisely the correct combination with the factor $N_3(i)^{1/3}$ needed to identify the leading terms with the corresponding terms in the Einstein-Hilbert action. In other words, only if these terms are present can we claim to have an effective field theory which has anything to do with the standard diffeomorphism-invariant gravitational theory in the continuum. This is neither automatic nor obvious, since our starting point involved both a discretization and an explicit asymmetry between space and time, and since the nonperturbative interplay of the local geometric excitations we are summing over in the path integral is beyond our analytic control. Nevertheless, what we have found is that at least the leading terms in the effective action we have derived dynamically admit an interpretation as the standard Einstein term, thus passing a highly nontrivial consistency test.

V. FLUCTUATIONS AROUND DE SITTER SPACE

We have shown that the action (19) gives a very good description of the measured shape $\bar{N}_3(i)$ of the extended universe. Furthermore, we have shown that by assuming that the three-volume fluctuations around $\bar{N}_3(i)$ are sufficiently small so that a quadratic approximation is valid, we can use the measured fluctuations to reconstruct the discretized version (19) of the minisuperspace action (17), where k_1 and $\tilde{k}_2$ are independent of the total four-volume N_4 used in the simulations. This certainly provides strong evidence that both the minisuperspace description of the dynamical behavior of the (expectation value of the) three-volume, and the semiclassical quadratic truncation for the description of the quantum fluctuations in the three-volume are essentially correct.

In the following we will test in more detail how well the actions (17) and (19) describe the data encoded in the covariance matrix $\hat{C}$. The correlation function was defined in the previous section by

$$C_{N_4}(i, i') = \langle \delta N_3(i) \delta N_3(i') \rangle, \qquad \delta N_3(i) \equiv N_3(i) - \bar{N}_3(i), \tag{39}$$

where we have included an additional subscript N_4 to

emphasize that N_4 is kept constant in a given simulation. The first observation extracted from the Monte Carlo simulations is that under a change in the four-volume $C_{N_4}(i, i')$ scales as[7]

$$C_{N_4}(i, i') = N_4 F(i/N_4^{1/4}, i'/N_4^{1/4}), \tag{40}$$

where F is a universal scaling function. This is illustrated by Fig. 8 for the rescaled version of the diagonal part $C_{N_4}^{1/2}(i, i)$, corresponding precisely to the quantum fluctuations $\langle(\delta N_3(i))^2\rangle^{1/2}$ of Fig. 1. While the height of the curve in Fig. 1 will grow as $N_4^{3/4}$, the superimposed fluctuations will only grow as $N_4^{1/2}$. We conclude that *for fixed bare coupling constants* the relative fluctuations will go to zero in the infinite-volume limit.

From the way the factor $\sqrt{N_4}$ appears as an overall scale in Eq. (20), it is clear that to the extent a quadratic expansion around the effective background geometry is valid, one will have a scaling

$$\langle \delta N_3(i) \delta N_3(i')\rangle = N_4^{3/2} \langle \delta n_3(t_i) \delta n_3(t_{i'})\rangle = N_4 F(t_i, t_{i'}), \tag{41}$$

where $t_i = i/N_4^{1/4}$. This implies that (40) provides additional evidence for the validity of the quadratic approximation and the fact that our choice of action (19), with k_1 independent of N_4, is indeed consistent.

To demonstrate in detail that the full function $F(t, t')$, and not only its diagonal part, is described by the effective actions (17) and (19), let us, for convenience, adopt a continuum language and compute its expected behavior. Expanding (17) around the classical solution according to $V_3(t) = V_3^{cl}(t) + x(t)$, the quadratic fluctuations are given by

$$\begin{aligned}\langle x(t)x(t')\rangle &= \int \mathcal{D}x(s)x(t)x(t')e^{-(1/2)\iint ds ds' x(s)M(s,s')x(s')} \\ &= M^{-1}(t, t'),\end{aligned} \tag{42}$$

where $\mathcal{D}x(s)$ is the normalized measure and the quadratic form $M(t, t')$ is determined by expanding the effective action S to second order in $x(t)$,

$$S(V_3) = S(V_3^{cl}) + \frac{1}{18\pi G}\frac{B}{V_4}\int \mathrm{d}t x(t)\hat{H}x(t). \tag{43}$$

In expression (43), $\hat{H}$ denotes the Hermitian operator

$$\hat{H} = -\frac{\mathrm{d}}{\mathrm{d}t}\frac{1}{\cos^3(t/B)}\frac{\mathrm{d}}{\mathrm{d}t} - \frac{4}{B^2\cos^5(t/B)}, \tag{44}$$

[7]We stress again that the form (40) is only valid in that part of the universe whose spatial extension is considerably larger than the minimal S^3 constructed from 5 tetrahedra. (The spatial volume of the stalk typically fluctuates between 5 and 15 tetrahedra.)

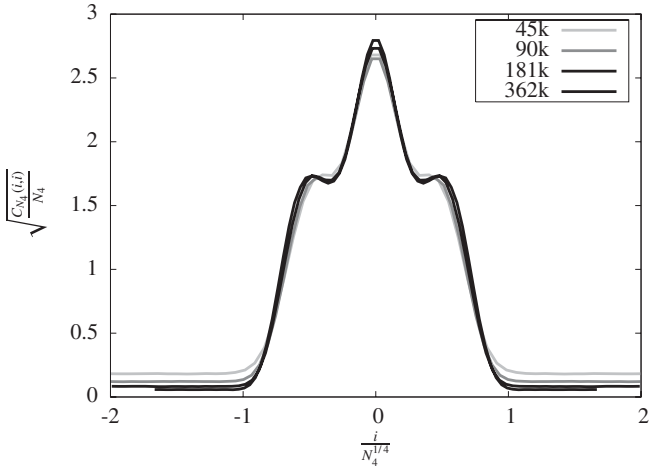

FIG. 8. Analysis of the quantum fluctuations of Fig. 1: diagonal entries $F(t, t)^{1/2}$ of the universal scaling function F from (40), for $N_4^{(4,1)} = 20.000$, 40.000, 80.000, and 160.000.

which must be diagonalized under the constraint that $\int dt\sqrt{g_{tt}}x(t) = 0$, since V_4 is kept constant.

Let $e^{(n)}(t)$ be the eigenfunctions of the quadratic form given by (43) with the volume constraint enforced,[8] ordered according to increasing eigenvalues λ_n. As we will discuss shortly, the lowest eigenvalue is $\lambda_1 = 0$, associated with translational invariance in time direction, and should be left out when we invert $M(t, t')$, because we precisely fix the center of volume when making our measurements. Its dynamics is therefore not accounted for in the correlator $C(t, t')$.

If this cosmological continuum model were to give the correct description of the computer-generated universe, the matrix

$$M^{-1}(t, t') = \sum_{n=2}^{\infty} \frac{e^{(n)}(t)e^{(n)}(t')}{\lambda_n} \tag{45}$$

should be proportional to the measured correlator $C(t, t')$. Figure 9 shows the eigenfunctions $e^{(2)}(t)$ and $e^{(4)}(t)$ (with two and four zeros, respectively), calculated from $\hat{H}$ with the constraint $\int dt\sqrt{g_{tt}}x(t) = 0$ imposed. Simultaneously we show the corresponding eigenfunctions calculated from the data, i.e. from the matrix $C(t, t')$, which correspond to the (normalizable) eigenfunctions with the highest and third-highest eigenvalues. The agreement is very good, in particular when taking into consideration that no parameter

[8]One simple way to find the eigenvalues and eigenfunctions approximately, including the constraint, is to discretize the differential operator, imposing that the (discretized) eigenfunctions vanish at the boundaries $t = \pm B\pi/2$, and finally adding the constraint as a term $\xi(\int dt x(t))^2$ to the action, where the coefficient ξ is taken large. The differential operator then becomes an ordinary matrix, and eigenvalues and eigenvectors can be found numerically. Stability with respect to subdivision and choice of ξ is easily checked.

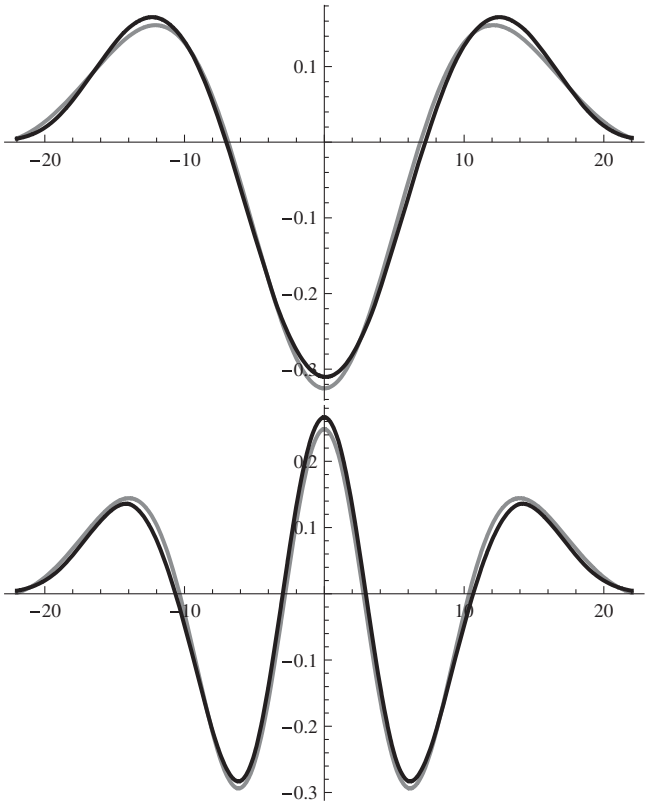

FIG. 9. Comparison of the two highest even eigenvectors of the covariance matrix $C(t, t')$ measured directly (gray curves) with the two lowest even eigenvectors of $M^{-1}(t, t')$, calculated semiclassically (black curves).

has been adjusted in the action [we simply take $B = s_0 N_4^{1/4} \Delta t$ in (14) and (43), which gives $B = 14.47 a_t$ for $N_4 = 362.000$].

The reader may wonder why the first eigenfunction exhibited has two zeros. As one would expect, the ground state eigenfunction $e^{(0)}(t)$ of the Hamiltonian (44), corresponding to the lowest eigenvalue, has no zeros, but it does not satisfy the volume constraint $\int dt \sqrt{g_{tt}} x(t) = 0$. The eigenfunction $e^{(1)}(t)$ of $\hat{H}$ with the next-lowest eigenvalue has one zero and is given by the simple analytic function

$$e^{(1)}(t) = \frac{4}{\sqrt{\pi B}} \sin\left(\frac{t}{B}\right) \cos^2\left(\frac{t}{B}\right) = c^{-1} \frac{dV_3^{cl}(t)}{dt}, \qquad (46)$$

where c is a constant. One realizes immediately that $e^{(1)}$ is the translational zero mode of the classical solution $V_3^{cl}(t)$ ($\propto \cos^3 t/B$). Since the action is invariant under time translations we have

$$S(V_3^{cl}(t + \Delta t)) = S(V_3^{cl}(t)), \qquad (47)$$

and since $V_3^{cl}(t)$ is a solution to the classical equations of motion we find to second order [using the definition (46)]

$$S(V_3^{cl}(t + \Delta t)) = S(V_3^{cl}(t)) + \frac{c^2 (\Delta t)^2}{18\pi G} \frac{B}{V_4} \times \int dt e^{(1)}(t) \hat{H} e^{(1)}(t), \qquad (48)$$

consistent with $e^{(1)}(t)$ having zero eigenvalue.

It is clear from Fig. 9 that some of the eigenfunctions of $\hat{H}$ (with the volume constraint imposed) agree very well with the measured eigenfunctions. All even eigenfunctions (those symmetric with respect to reflection about the symmetry axis located at the center of volume) turn out to agree very well. The odd eigenfunctions of $\hat{H}$ agree less well with the eigenfunctions calculated from the measured $C(t, t')$. The reason seems to be that we have not managed to eliminate the motion of the center of volume completely from our measurements. As already mentioned above, there is an inherent ambiguity in fixing the center of volume, which turns out to be sufficient to reintroduce the zero mode in the data. Suppose we had by mistake misplaced the center of volume by a small distance Δt. This would introduce a modification

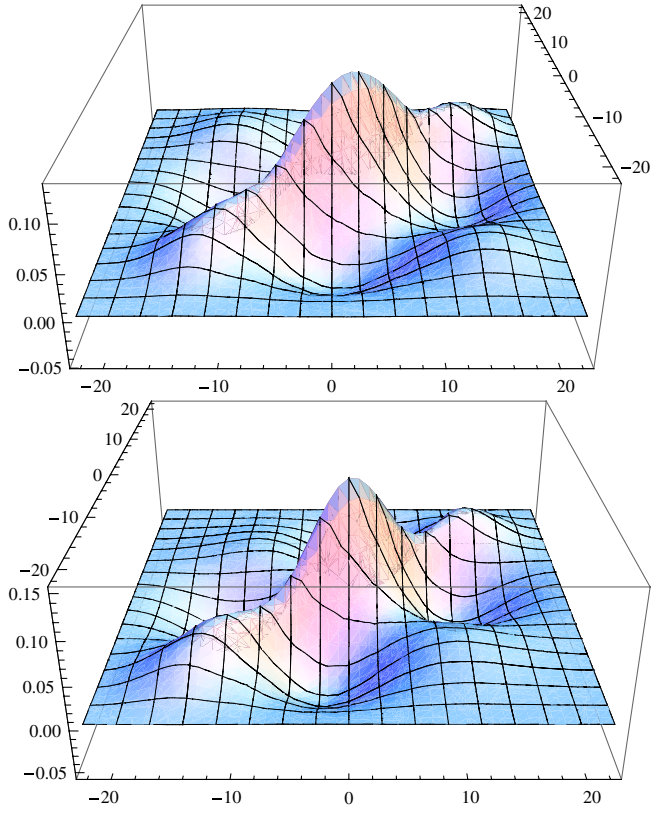

FIG. 10 (color online). Comparison of data for the extended part of the universe: measured $C(t, t')$ (upper panel) versus $M^{-1}(t, t')$ obtained from analytical calculation (lower panel). The agreement is good, and would have been even better had we included only the even modes.

$$\Delta V_3 = \frac{dV_3^{cl}(t)}{dt}\Delta t \tag{49}$$

proportional to the zero mode of the potential $V_3^{cl}(t)$. It follows that the zero mode can reenter whenever we have an ambiguity in the position of the center of volume. In fact, we have found that the first odd eigenfunction extracted from the data can be perfectly described by a linear combination of $e^{(1)}(t)$ and $e^{(3)}(t)$. It may be surprising at first that an ambiguity of one lattice spacing can introduce a significant mixing. However, if we translate ΔV_3 from Eq. (49) to "discretized" dimensionless units using $V_3(i) \sim N_4^{3/4}\cos(i/N_4^{1/4})$, we find that $\Delta V_3 \sim \sqrt{N_4}$, which because of $\langle(\delta N_3(i))^2\rangle \sim N_4$ is of the same order of magnitude as the fluctuations themselves. In our case, this apparently does affect the odd eigenfunctions.

One can also compare the data and the matrix $M^{-1}(t, t')$ calculated from (45) directly. This is illustrated in Fig. 10, where we have restricted ourselves to data from inside the extended part of the universe. We imitate the construction (45) for M^{-1}, using the data to calculate the eigenfunctions, rather than $\hat{H}$. One could also have used $C(t, t')$ directly, but the use of the eigenfunctions makes it somewhat easier to perform the restriction to the bulk. The agreement is again good (better than 15% at any point on the plot), although less spectacular than in Fig. 9 because of the contribution of the odd eigenfunctions to the data.

VI. THE GEOMETRY OF SPATIAL THREE-SPHERES

We have shown above that our data for the spatial three-volumes have a natural interpretation as coming from the slicing of a four-sphere with standard geometry (the "round" four-sphere), with relatively small quantum fluctuations superimposed. It is natural to ask to what extent the spatial three-spheres themselves can be assigned the standard geometry of a round three-sphere, again with relatively small quantum fluctuations superimposed. We have already provided evidence that the Hausdorff dimension of the spatial slices is three [4,5]. However, the Hausdorff dimension is a very coarse measure of geometry, and even very fractal structures can have Hausdorff dimension three.[9]

We have analyzed the geometry of the spatial three-spheres as follows. Each spatial slice at integer proper time i is a triangulation, consisting of a certain number N_3 of tetrahedra, glued together pairwise such that the resulting topology is that of a three-sphere. We now choose an arbitrary tetrahedron as the origin of measurements and subsequently decompose the S^3 into (thick) shells of tetrahedra characterized by their distance r from this origin, where the distance r is defined as the minimal number of tetrahedra one has to cross when moving from the shell to the origin via neighboring tetrahedra. We call the number of tetrahedra in the shell at distance r the *area* $A(r, N_3)$ of the shell. In order to compute the expectation value of this quantity, we have to repeat the measurements in a way that averages over different triangulations of S^4, over different spatial slices within the S^4's, and over different locations of the point of origin within those slices. In this manner we can test whether $\langle A(r, N_3)\rangle$ behaves like a regular three-sphere (with only small fluctuations superimposed), with r viewed as the geodesic distance. If this was the case, one would expect a functional dependence of the form

$$\langle A(r, N_3)\rangle \propto N_3^{2/3}\sin^2\left(\frac{r}{cN_3^{1/3}}\right), \tag{50}$$

with c a constant.

Figure 11 summarizes the results of our measurements. Since we are not interested in very small N_3's where no continuum scaling is expected, we have restricted ourselves to spatial slices close to the center of volume as defined above, where N_3 is largest. The first thing to note about Fig. 11 is that the data from spatial slices at different distances from the center of volume fall to good accuracy on a common, universal curve. Next, we observe that relation (50) is reasonably well satisfied, except for the measurements at large radii r, which exhibit a tail not described by formula (50). This signals the presence of large fluctuations in the geometry (the shape) of the spatial slices to the effect that we cannot simply view them—in the sense of expectation values—as classical spheres of constant positive curvature with fixed radius proportional to $N^{1/3}$, superimposed by small quantum fluctuations. In

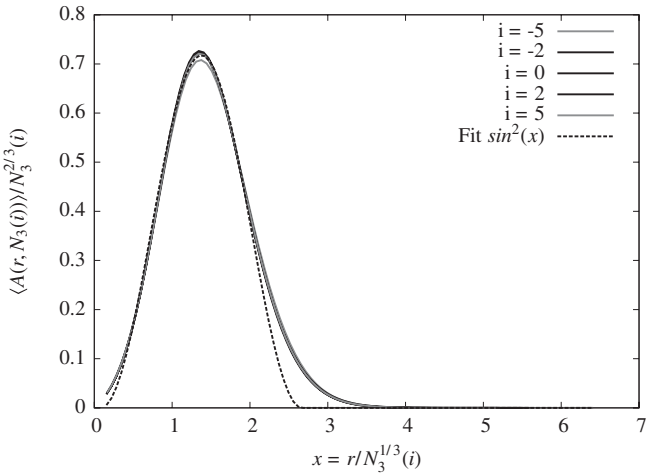

FIG. 11. Testing relation (50) for the bare coupling constants $\kappa_0 = 2.2$ and $\Delta = 0.6$, at four-volume $N_4^{(4,1)} = 160.000$. Data have been collected for spatial slices at various distances close to the center of volume.

[9]To illustrate the point, the Hausdorff dimension of the complex plane (with standard geometry) is of course equal to two, but the same is true for the highly fractal structure of so-called branched polymers or planar trees embedded in the plane.

fact, there is already evidence that the geometry, when defined with respect to the geodesic distance r, has certain fractal properties [4]. This can be substantiated and quantified by measuring the topology of a typical spherical shell at a distance r from a chosen origin in more detail. At sufficiently large radius r one finds that the topology is no longer that of a single two-sphere, but branches out into a number of disconnected pieces, most likely by effectively creating a number of spatial "baby universes." It is well known how to study the distribution of such baby universes [22,23], and we believe that these methods will yield a quantitative description of the observed slower falloff for large r. Details of this picture, including a study of the temporal dynamics of such spatial baby universes, will be published elsewhere.

VII. THE SIZE OF THE UNIVERSE AND THE FLOW OF G

Let us now return to Eq. (21),

$$G = \frac{a^2}{k_1}\frac{\sqrt{\tilde{C}_4}\tilde{s}_0^2}{3\sqrt{6}}, \tag{51}$$

which relates the parameter k_1 extracted from the Monte Carlo simulations to Newton's constant in units of the cutoff a, G/a^2. For the bare coupling constants $(\kappa_0, \Delta) = (2.2, 0.6)$ we have high-statistics measurements for N_4 ranging from 45.500 to 362.000 four-simplices (equivalently, $N_4^{(4,1)}$ ranging from 20.000 to 160.000 four-simplices). The choice of Δ determines the asymmetry parameter α, and the choice of (κ_0, Δ) determines the ratio ξ between $N_4^{(3,2)}$ and $N_4^{(4,1)}$. This in turn determines the "effective" four-volume $\tilde{C}_4$ of an average four-simplex, which also appears in (51). The number $\tilde{s}_0$ in (51) is determined directly from the time extension T_{univ} of the extended universe according to

$$T_{\text{univ}} = \pi\tilde{s}_0(N_4^{(4,1)})^{1/4}. \tag{52}$$

Finally, from our measurements we have determined $k_1 = 0.038$. Taking everything together according to (51), we obtain $G \approx 0.23a^2$, or $\ell_{\text{Pl}} \approx 0.48a$, where $\ell_{\text{Pl}} = \sqrt{G}$ is the Planck length.

From the identification of the volume of the four-sphere, $V_4 = 8\pi^2R^4/3 = \tilde{C}_4N_4^{(4,1)}a^4$, we obtain that $R = 3.1a$. In other words, the linear size πR of the quantum de Sitter universes studied here lies in the range of 12–21 Planck lengths for N_4 in the range mentioned above and for the bare coupling constants chosen as $(\kappa_0, \Delta) = (2.2, 0.6)$.[10]

[10]Small deviations from the corresponding numbers quoted in [7] have their origin in the more careful (and correct) treatment of the various four-volumes N_4, $N_4^{(4,1)}$, and $N_4^{(3,2)}$ in the present work.

Our dynamically generated universes are therefore not very big, and the quantum fluctuations around their average shape are large as is apparent from Fig. 1. It is rather surprising that the semiclassical minisuperspace formulation is applicable for universes of such a small size, a fact that should be welcome news to anyone performing semiclassical calculations to describe the behavior of the early universe. However, in a certain sense our lattices are still coarse compared to the Planck scale ℓ_{Pl} because the Planck length is roughly half a lattice spacing. If we are after a theory of quantum gravity valid on all scales, we are, in particular, interested in uncovering phenomena associated with Planck-scale physics. In order to collect data free from unphysical short-distance lattice artifacts at this scale, we would ideally like to work with a lattice spacing much smaller than the Planck length, while still being able to set by hand the physical volume of the universe studied on the computer.

The way to achieve this, under the assumption that the coupling constant G of formula (51) is indeed a true measure of the gravitational coupling constant, is as follows. We are free to vary the discrete four-volume N_4 and the bare coupling constants (κ_0, Δ) of the Regge action (see [4] for further details on the latter). Assuming for the moment that the semiclassical minisuperspace action is valid, the effective coupling constant k_1 in front of it will be a function of the bare coupling constants (κ_0, Δ), and can, in principle, be determined as described above for the case $(\kappa_0, \Delta) = (2.2, 0.6)$. If we adjusted the bare coupling constants such that in the limit as $N_4 \to \infty$ both

$$V_4 \sim N_4a^4 \quad \text{and} \quad G \sim a^2/k_1(\kappa_0, \Delta) \tag{53}$$

remained constant [i.e. $k_1(\kappa_0, \Delta) \sim 1/\sqrt{N_4}$], we would eventually reach a region where the Planck length was significantly smaller than the lattice spacing a, in which event the lattice could be used to approximate spacetime structures of Planckian size and we could initiate a genuine study of the sub-Planckian regime. Since we have no control over the effective coupling constant k_1, the first obvious question which arises is whether we can at all adjust the bare coupling constants in such a way that at large scales we still see a four-dimensional universe, with k_1 going to zero at the same time. The answer seems to be in the affirmative, as we will go on to explain.

Figure 12 shows the results of extracting k_1 for a range of bare coupling constants for which we still observe an extended universe. In the top figure $\Delta = 0.6$ is kept constant while κ_0 is varied. For κ_0 sufficiently large we eventually reach a point where a phase transition takes place (the point in the square in the bottom right-hand corner is the measurement closest to the transition we have looked at). For even larger values of κ_0, beyond this transition, the universe disintegrates into a number of small universes, in a CDT analogue of the branched-polymer

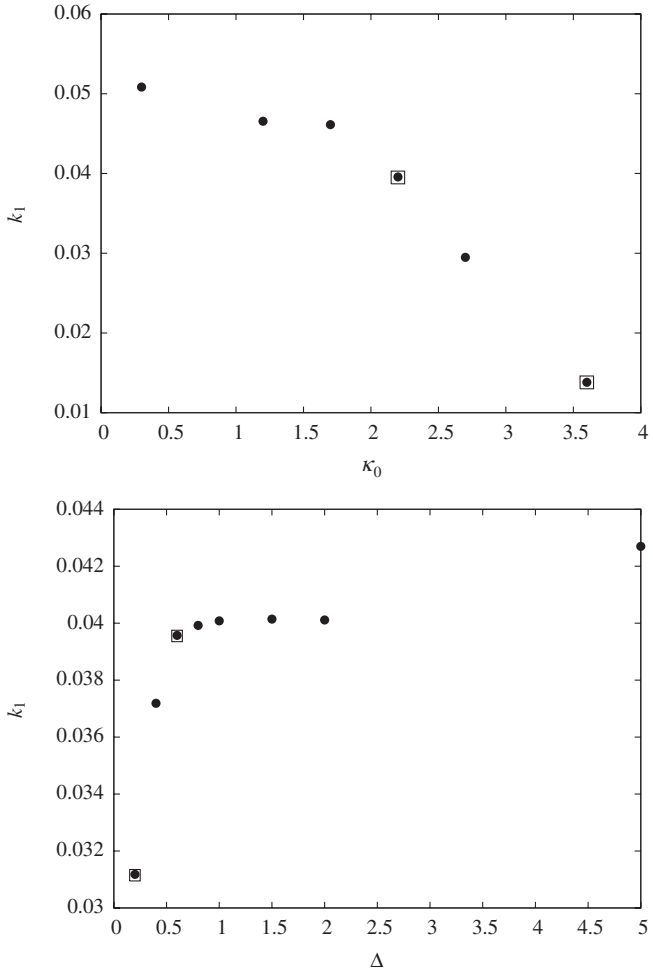

FIG. 12. The measured effective coupling constant k_1 as a function of the bare κ_0 (top panel, $\Delta = 0.6$ fixed) and the asymmetry Δ (bottom panel, $\kappa_0 = 2.2$ fixed). The marked point near the middle of the data points sampled is the point $(\kappa_0, \Delta) = (2.2, 0.6)$ where most measurements in the remainder of the paper were taken. The other marked points are those closest to the two phase transitions, to the "branched-polymer phase" (top panel) and the "crumpled phase" (bottom panel).

phase of Euclidean quantum gravity. The plot shows that the effective coupling constant k_1 becomes smaller and possibly goes to zero as the phase transition point is approached, although our current data do not yet allow us to conclude that k_1 does indeed vanish at the transition point.

Conversely, the bottom panel of Fig. 12 shows the effect of varying Δ while keeping $\kappa_0 = 2.2$ fixed. As Δ is decreased towards 0, we eventually hit another phase transition, separating the physical phase of extended universes from the CDT equivalent of the crumpled phase of Euclidean quantum gravity, where the entire universe will be concentrated within a few time steps, as already mentioned in Sec. III above. (The point closest to the transition where we have taken measurements is the one in the bottom left-hand corner.) Also, when approaching this phase transition the effective coupling constant k_1 goes to 0, leading to the tentative conclusion that $k_1 \to 0$ along the entire phase boundary.

However, to extract the coupling constant G from (51) we not only have to take into account the change in k_1, but also that in $\tilde{s}_0$ [the width of the distribution $N_3(i)$] and in the effective four-volume $\tilde{C}_4$ as a function of the bare coupling constants. Combining these changes, we arrive at a slightly different picture. Approaching the boundary where spacetime collapses in time direction (by lowering Δ), the gravitational coupling constant G *decreases*, despite the fact that $1/k_1$ increases. This is a consequence of $\tilde{s}_0$ decreasing considerably, as can be seen from Fig. 3. On the other hand, when (by increasing κ_0) we approach the region where the universe breaks up into several independent components, the effective gravitational coupling constant G increases, more or less like $1/k_1$, where the behavior of k_1 is shown in Fig. 12 (top panel). This implies that the Planck length $\ell_{\rm Pl} = \sqrt{G}$ increases from approximately $0.48a$ to $0.83a$ when κ_0 changes from 2.2 to 3.6. Most likely we can make it even bigger in terms of Planck units by moving closer to the phase boundary.

On the basis of these arguments, it seems likely that the nonperturbative CDT formulation of quantum gravity does allow us to penetrate into the sub-Planckian regime and probe the physics there explicitly. Work in this direction is currently ongoing. One interesting issue under investigation is whether and to what extent the simple minisuperspace description remains valid as we go to shorter scales. We have already seen deviations from classicality at short scales when measuring the spectral dimension [4,20], and one would expect them to be related to additional terms in the effective action (17) and/or a nontrivial scaling behavior of k_1. This raises the interesting possibility of being able to test explicitly the scaling violations of G predicted by renormalization group methods in the context of asymptotic safety [2].

VIII. DISCUSSION

The CDT model of quantum gravity is extremely simple. It is the path integral over the class of causal geometries with a global time foliation. In order to perform the summation explicitly, we introduce a grid of piecewise linear geometries, much in the same way as when defining the path integral in quantum mechanics. Next, we rotate each of these geometries to Euclidean signature and use as a bare action the Einstein-Hilbert action[11] in Regge form. That is all.

The resulting superposition exhibits a nontrivial scaling behavior as a function of the four-volume, and we observe

[11]Of course, the full, effective action, including measure contributions, will contain all higher-derivative terms.

the appearance of a well-defined average geometry, that of de Sitter space, the maximally symmetric solution to the classical Einstein equations in the presence of a positive cosmological constant. We are definitely in a quantum regime, since the fluctuations of the three-volume around de Sitter space are sizable, as can be seen in Fig. 1. Both the average geometry and the quantum fluctuations are well described in terms of the minisuperspace action (17). A key feature to appreciate is that, unlike in standard (quantum-) cosmological treatments, this description is the *outcome* of a nonperturbative evaluation of the *full* path integral, with everything but the scale factor [equivalently, $V_3(t)$] summed over. Measuring the correlations of the quantum fluctuations in the computer simulations for a particular choice of bare coupling constants enabled us to determine the continuum gravitational coupling constant G as $G \approx 0.42a^2$, thereby introducing an absolute physical length scale into the dimensionless lattice setting. Within measuring accuracy, our de Sitter universes (with volumes lying in the range of 6.000–47.000 ℓ_{Pl}^4) are seen to behave perfectly semiclassically with regard to their large-scale properties.

We have also indicated how we may be able to penetrate into the sub-Planckian regime by suitably changing the bare coupling constants. By ''sub-Planckian regime'' we mean that the lattice spacing a is (much) smaller than the Planck length. While we have not yet analyzed this region in detail, we expect to eventually observe a breakdown of the semiclassical approximation. This will hopefully allow us to make contact with attempts to use renormalization group techniques in the continuum and the concept of asymptotic safety to study scaling violations in quantum gravity [2].

On the basis of the results presented here, two major issues suggest themselves for further research. First, we need to establish the relation of our effective gravitational coupling constant G with a more conventional gravitational coupling constant, defined directly in terms of coupling matter to gravity. In the present work, we have defined G as the coupling constant in front of the effective action, but it would be desirable to verify directly that a gravitational coupling defined via the coupling to matter agrees with our G. In principle, it is easy to couple matter to our model, but it is less straightforward to define in a simple way a setup for extracting the semiclassical effect of gravity on the matter sector. Attempts in this direction were already undertaken in the ''old'' Euclidean approach [24,25], and it is possible that similar ideas can be used in CDT-quantum gravity. Work on this is in progress.

The second issue concerns the precise nature of the ''continuum limit.'' Recall our discussion in the Introduction about this in a conventional lattice-theoretic setting. The continuum limit is usually linked to a divergent correlation length at a critical point. It is unclear whether such a scenario is realized in our case. In general, it is rather unclear how one could define at all the concept of a divergent length related to correlators in quantum gravity, since one is integrating over all geometries, and it is the geometries which dynamically give rise to the notion of ''length.''

This has been studied in detail in two-dimensional (Euclidean) quantum gravity coupled to matter with central charge $c \leq 1$ [26]. It led to the conclusion that one could associate the critical behavior of the matter fields (i.e. approaching the critical point of the Ising model) with a divergent correlation length, although the matter correlators themselves had to be defined as nonlocal objects due to the requirement of diffeomorphism invariance. On the other hand, the two-dimensional studies do not give us a clue of how to treat the gravitational sector itself, since they do not possess gravitational field-theoretic degrees of freedom. What happens in the two-dimensional lattice models which can be solved analytically is that the only fine-tuning needed to approach the continuum limit is an additive renormalization of the cosmological constant (for fixed matter couplings). Thus, fixing the two-dimensional spacetime volume N_2 (the number of triangles), such that the cosmological constant plays no role, there are no further coupling constants to adjust and the continuum limit is automatically obtained by the assignment $V_2 = N_2 a^2$ and taking $N_2 \to \infty$. This situation can also occur in special circumstances in ordinary lattice field theory. A term like

$$\sum_i c_1(\phi_{i+1} - \phi_i)^2 + c_2(\phi_{i+1} + \phi_{i-1} - 2\phi_i)^2 \qquad (54)$$

(or a higher-dimensional generalization) will also go to the continuum free field theory simply by increasing the lattice size and using the identification $V_d = L^d a^d$ (L denoting the linear size of the lattice in lattice units), the higher-derivative term being subdominant in the limit. It is not obvious that in quantum gravity one can obtain a continuum quantum field theory without fine-tuning in a similar way, because the action in this case is multiplied by a dimensionful coupling constant. Nevertheless, it is certainly remarkable that the infrared limit of our effective action apparently reproduces—within the cosmological setting—the Einstein-Hilbert action, which is the unique diffeomorphism-invariant generalization of the ordinary kinetic term, containing at most second derivatives of the metric. A major question is whether and how far our theory can be pushed towards an ultraviolet limit. We have indicated how to obtain such a limit by varying the bare coupling constants of the theory, but the investigation of the limit $a \to 0$ with fixed G has only just begun.

ACKNOWLEDGMENTS

All authors acknowledge support by ENRAGE (European Network on Random Geometry), a Marie Curie Research Training Network, Contract No. MRTN-CT-2004-005616, and A. G. and J. J. by COCOS

(Correlations in Complex Systems), a Marie Curie Transfer of Knowledge Project, Contract No. MTKD-CT-2004-517186, both in the European Community's Sixth Framework Programme. R. L. acknowledges support by the Netherlands Organisation for Scientific Research (NWO) under their VICI program.

[1] S. Weinberg, in *General Relativity: Einstein Centenary Survey*, edited by S. W. Hawking and W. Israel (Cambridge University Press, Cambridge, England, 1979), pp. 790–831.
[2] A. Codello, R. Percacci, and C. Rahmede, arXiv:0805.2909; M. Reuter and F. Saueressig, arXiv:0708.1317; M. Niedermaier and M. Reuter, Living Rev. Relativity **9**, 5 (2006); H. W. Hamber and R. M. Williams, Phys. Rev. D **72**, 044026 (2005); D. F. Litim, Phys. Rev. Lett. **92**, 201301 (2004); H. Kawai, Y. Kitazawa, and M. Ninomiya, Nucl. Phys. **B467**, 313 (1996).
[3] J. Ambjørn, J. Jurkiewicz, and R. Loll, Nucl. Phys. **B610**, 347 (2001).
[4] J. Ambjørn, J. Jurkiewicz, and R. Loll, Phys. Rev. D **72**, 064014 (2005).
[5] J. Ambjørn, J. Jurkiewicz, and R. Loll, Phys. Rev. Lett. **93**, 131301 (2004).
[6] J. Ambjørn, J. Jurkiewicz, and R. Loll, Phys. Lett. B **607**, 205 (2005).
[7] J. Ambjørn, A. Görlich, J. Jurkiewicz, and R. Loll, Phys. Rev. Lett. **100**, 091304 (2008).
[8] J. Ambjørn, J. Jurkiewicz, and R. Loll, arXiv:0806.0397.
[9] C. Teitelboim, Phys. Rev. Lett. **50**, 705 (1983); Phys. Rev. D **28**, 297 (1983).
[10] J. Ambjørn, J. Jurkiewicz, and R. Loll, Contemp. Phys. **47**, 103 (2006); R. Loll, Classical Quantum Gravity **25**, 114006 (2008).
[11] J. Ambjørn and R. Loll, Nucl. Phys. **B536**, 407 (1998).
[12] J. Ambjørn, R. Loll, W. Westra, and S. Zohren, J. High Energy Phys. 12 (2007) 017; J. Ambjørn, R. Loll, Y. Watabiki, W. Westra, and S. Zohren, J. High Energy Phys. 05 (2008) 032; Phys. Lett. B **665**, 252 (2008).
[13] J. Ambjørn, J. Jurkiewicz, R. Loll, and G. Vernizzi, J. High Energy Phys. 09 (2001) 022; Acta Phys. Pol. B **34**, 4667 (2003); J. Ambjørn, J. Jurkiewicz, and R. Loll, Phys. Lett. B **581**, 255 (2004).
[14] D. Benedetti, R. Loll, and F. Zamponi, Phys. Rev. D **76**, 104022 (2007).
[15] J. Ambjørn, B. Durhuus, and J. Fröhlich, Nucl. Phys. **B257**, 433 (1985); J. Ambjørn, B. Durhuus, J. Fröhlich, and P. Orland, Nucl. Phys. **B270**, 457 (1986).
[16] A. Billoire and F. David, Phys. Lett. **168B**, 279 (1986).
[17] D. V. Boulatov, V. A. Kazakov, I. K. Kostov, and A. A. Migdal, Nucl. Phys. **B275**, 641 (1986).
[18] J. Ambjørn and J. Jurkiewicz, Phys. Lett. B **278**, 42 (1992).
[19] M. E. Agishtein and A. A. Migdal, Mod. Phys. Lett. A **7**, 1039 (1992).
[20] J. Ambjørn, J. Jurkiewicz, and R. Loll, Phys. Rev. Lett. **95**, 171301 (2005).
[21] B. Dittrich and R. Loll, Classical Quantum Gravity **23**, 3849 (2006).
[22] J. Ambjørn, S. Jain, J. Jurkiewicz, and C. F. Kristjansen, Phys. Lett. B **305**, 208 (1993).
[23] J. Ambjørn, S. Jain, and G. Thorleifsson, Phys. Lett. B **307**, 34 (1993).
[24] B. V. de Bakker and J. Smit, Nucl. Phys. **B484**, 476 (1997).
[25] H. W. Hamber and R. M. Williams, Nucl. Phys. **B435**, 361 (1995).
[26] J. Ambjørn, K. N. Anagnostopoulos, U. Magnea, and G. Thorleifsson, Phys. Lett. B **388**, 713 (1996); J. Ambjørn and K. N. Anagnostopoulos, Nucl. Phys. **B497**, 445 (1997); J. Ambjørn, K. N. Anagnostopoulos, and R. Loll, Phys. Rev. D **60**, 104035 (1999).